

Performance of ERA-Interim wave data in the nearshore waters around India

Sanil Kumar V*, Muhammed Naseef T

Ocean Engineering, CSIR-National Institute of Oceanography (Council of Scientific & Industrial Research), Dona Paula, Goa - 403 004 India

*Corresponding author: Tel: 0091 832 2450 327 Fax: 0091 832 2450 602 Email: sanil@nio.org

Abstract

Bulk wave parameters such as wave height and wave period are required for engineering and environmental applications. In this study, measured wave data from six shallow water locations in the data-sparse North Indian Ocean are used to assess the European Centre for Medium-Range Weather Forecasts (ECMWF) Interim Re-Analysis (ERA-I) wave height and period data in the nearshore waters around India. The difference between the ERA-I significant wave height (SWH) and the buoy SWH varies from -1 to 1 m with an average value of -0.1 m for the three west coast locations. For the three east coast locations, the variation ranges from -2.2 to 1.7 m with an average value of -0.2 m. The ERA-I SWH data shows positive biases, indicating an overall overestimation for all locations except for the northern location in the west coast of India where underestimation is observed. During the tropical cyclone period, a large (~33%) underestimation of SWH in the ERA-I data is observed. Hence, the ERA-I SWH data cannot be used for design applications without site-specific validation. The difference between the wave period from ERA-I and the energy wave period from the buoy varies from -6 to 4 s with an average value of -0.3 s. The inter-comparisons suggest that the ERA-I dataset shows encouraging agreement with the annual-mean SWH and the energy wave period.

Key words: *Surface waves, reanalysis, buoy observation, Indian Ocean, ECMWF, ERA-Interim, wave height, wave period*

1. Introduction

Wind waves are a prominent feature of the ocean surface and play a major role in activity planning in the open ocean and in coastal zones (Tucker and Pitt 2001). The monsoons of the Indian Ocean are an example of strong ocean-atmosphere interaction over basin scales. The Arabian Sea (AS) and the Bay of Bengal (BoB) play an important role in modulating the monsoons over the Indian Ocean. Bounded to the north by the Asian continent, the unique geography of the North Indian Ocean leads to a complex annual cycle associated with substantial seasonal reversals of the annual monsoon winds (Slingo et al. 2005). The reversal of the large-scale wind field in the northern Indian Ocean between the boreal summer and winter leads to seasonal changes in waves. Near shore region of east coast of India is very steep and narrow, whereas it is broad and flat in the west coast of India. The effect of summer monsoon is higher in the west coast compared to that in the east coast of India. North Indian Ocean is frequented by cyclonic storms and the impact of cyclonic storm is higher in the BoB than in the AS (Singh et al. 2000) and these events can cause inter-annual variations in wave parameters (Shanas and Kumar 2015). Cyclones in the BoB generally occur in April–May and October–December.

Generally, wave characteristics are represented by significant wave height (SWH) and wave period (T). Wave data at a location are obtained through i) in-situ measurements, ii) voluntary observing ships (VOS) data, iii) satellite altimeter and iv) model datasets. In-situ wave data coverage in the North Indian Ocean is sparse. For most of the area, it is not available for a long duration due to the high expense of the installation and maintenance of wave measuring instruments. Visual observations of wave parameters from ships (VOS) data have been available along shipping routes since 1784. However, by their nature these observations are subjective and there are large un-sampled areas over the oceans due to missing ship routes (Gulev and Grigorieva, 2004). Satellite altimetry and its recent improvement in resolution as well as in data quality are worthwhile, but globally, the repeat cycle of satellite altimetry for a location varies from 10 days for TOPEX/POSEIDON satellite mission to 35 days for ERS satellites (Traon 2013). Hence, satellite altimetry does not present high temporal resolution and the chances of missing extreme events are high.

Wave hind-casts with numerical models have become a common tool to get the wave height and wave period for locations devoid of observational data. The data based on the numerical model require validation before using for practical application. Vethamony et al. (2006) compared the numerical model

(MIKE 21) results with measured buoy data in the North Indian Ocean. They reported the correlation coefficients for the model and measured significant wave heights (SWHs) in the range 0.68-0.91 m with a bias up to 0.6 m. At some locations during the south-west (SW) monsoon period, the difference between the measured SWH and the model SWH is up to 2 m (Vethamony et al. 2006). The hindcasts of wave parameters in the Indian Ocean using MIKE 21 SW by Remya et al. (2012) showed a difference of up to 1.5 m between the model SWH and the measured SWH.

The ERA-Interim (hereafter ERA-I) dataset is available for all locations of the globe from 1979. Recently, a validation study was carried out by comparing ERA-I data with buoy data (Stopa and Cheung 2014). Stopa and Cheung (2014) observed that ERA-I data generally underestimates the wave height with lower standard deviations in comparison to observations, but it maintains slightly better error metrics. Some studies around the globe have been conducted on the correction of the reanalysis product (Caires and Sterl 2005). However, the accuracy of the ERA-I SWH and wave period in the data-sparse North Indian Ocean is not well documented. Shanas and Kumar (2014a) compared the ERA-I wave parameters with buoy data at a shallow water location and a deep water location in the eastern AS for a few days during the high wave condition (SWH > 2 m). They found that the maximum SWH based on ERA-I data in deep water is 15% less than the maximum SWH measured by the buoy. They also found that, in shallow water, ERA-I overpredicts the maximum SWH by 9%. Finally, Shanas and Kumar (2014a) found that the comparison of the wave period and direction at both locations shows significant scattering.

The ERA-I dataset is widely used i) for arriving at the design wave condition (Agarwal et al. 2013), ii) studying the long-term variation in wave height (Shanas and Kumar 2014b) and iii) assessing the wave power potential (Portilla et al. 2013). Hence, it is important to know how this dataset compares with measured wave data during different seasons and at different locations. In this study, the ERA-I wave height and wave period data were compared with buoy measured data at six shallow water locations in the North Indian Ocean. Three of the locations were off the west coast of India and three were off the east coast of India (Figure 1). Table 1 provides the details of the locations and the periods of the data used in the analysis. The wave characteristics of the study locations are presented in Sajiv et al. (2012), Glejin et al. (2013a; 2013b), Anoop et al. (2014), Kumar et al. (2014a; 2014b), Dora and Kumar (2015) and Kumar and Anjali (2015). The overall data that was considered and the associated methodology for

their processing are presented in Section 2. The presentation and analysis of the results are reported in Section 3, and the summary and conclusions are presented in Section 4.

2. Data and method

a. ERA-Interim data

The SWH and wave period (T) from the ERA-Interim Global Atmospheric Reanalysis produced by the European Centre for Medium-Range Weather Forecasts (ECMWF) was used in the study (http://apps.ecmwf.int/datasets/data/interim_full_daily/). The ECMWF Interim Re-Analysis (ERA-I) is the latest ECMWF global reanalysis coupling atmosphere and surface waves and providing data at a spatial resolution of 1.5° and a temporal resolution of 6 h (Dee et al. 2011). An updated atmospheric model (the Integrated Forecast System Cycle 31r2 or IFS) was used in the data analysis. ERA-I uses recent satellite altimeter data together with built-in ERA-40 data assimilation. The wave model incorporated in the IFS is based on the WAM approach (Komen et al. 1994), and the version used in ERA-I includes several enhancements, both in physics and numerics, over the version that was used in ERA-40. Also, the wave model used in ERA-I includes shallow water physics (Janssen et al. 2005; Janssen 2008). The updated version of WAM includes a revised formulation of ocean wave dissipation, which has reduced the root mean square error in the wave period against the buoy data and shows that the error in the estimate of wave period are much smaller than that in ERA-40 (Bidlot et al. 2007).

b. Buoy data

The measured wave data using the directional wave rider buoy, DWR Mk-III, was compared with ERA-I wave data. The wave measurements were carried out by the National Institute of Oceanography (Council of Scientific & Industrial Research, Govt. of India) and the Indian National Centre for Ocean Information Services (Ministry of Earth Sciences, Govt. of India) as part of the project “Real-time wave data collection in the Indian waters for Coastal Ocean Forecast.” The directional wave rider buoy measures free surface gravity waves with heaves in the range of -20 and +20 m, with a resolution of 1 cm in heaves and range of wave periods between 1.6 and 30 s. The cross-sensitivity of the heaves is less than 3%. Data were recorded continuously at 1.28 Hz interval, and the data for every 30 min were processed as one record. The details of the data analysis are presented in Kumar et al. (2014a). The collected time series was subjected to standard error verification for spikes, steepness and constant signals. The wave spectrum was computed from the measured time series of the heave motion of the

buoy using fast Fourier transform. The frequency resolution was 0.005 Hz for frequencies less than 0.1 Hz and 0.01 Hz otherwise. The significant wave height (SWH) and the energy wave period (T_e) were obtained from the spectral moments as shown in Equations 1 and 2. From the measured half-hour record, the records at 6-hour intervals were used for comparison with the ERA-I data.

$$\text{Significant wave height (SWH)} = 4\sqrt{m_0} \quad (1)$$

$$\text{Energy wave period } (T_e) = \frac{m_{-1}}{m_0} \quad (2)$$

where m_n is the n th order spectral moment and given by $m_n = \int_0^\infty f^n S(f) df$, $n=0$ and -1 , and $S(f)$ is the spectral energy density at frequency f .

c. Statistical parameters used for data comparison

The statistical parameters used for comparison of the ERA-I data with the measured wave data were the root-mean-square error (RMSE), bias, scattering index (SI) and correlation coefficient (r) and are defined below.

$$\text{RMSE} = \sqrt{\frac{1}{N} \sum_{i=1}^N (A_i - B_i)^2} \quad (3)$$

$$\text{Bias} = \frac{1}{N} \sum_{i=1}^N (A_i - B_i) \quad (4)$$

$$\text{SI} = \frac{\sqrt{\frac{1}{N} \sum_{i=1}^N [(A_i - \bar{A}) - (B_i - \bar{B})]^2}}{\bar{B}} \quad (5)$$

$$r = \frac{N \sum_{i=1}^N A_i B_i - \sum_{i=1}^N A_i \sum_{i=1}^N B_i}{\sqrt{\left[N \sum_{i=1}^N A_i^2 - \left(\sum_{i=1}^N A_i \right)^2 \right] \left[N \sum_{i=1}^N B_i^2 - \left(\sum_{i=1}^N B_i \right)^2 \right]}} \quad (6)$$

where A_i represents the data obtained from the ERA-I, B_i represents the data from the buoy measurements, N is the number of data points and the over bar represents the mean value.

The bias is a statistical quantity that signifies the average difference between the ERA-I and buoy data. The lower value of RMSE indicates a better fit of data between ERA-I and observations.

3. Results and discussions

a. Significant wave height

The measured buoy data shows that the annual mean SWH along the eastern AS is 1 to 1.1 m, whereas the annual mean SWH along the western BoB is 0.7 to 1.3 m (Table 2). Along the eastern AS, the variation in SWH between Karwar and Ratnagiri is equal to or slightly greater than 20% during the non-monsoon period, whereas it is less than 10% during the monsoon season (Anoop et al. 2014). Due to the SW monsoon influence in the eastern AS, the monthly mean SWH varies from 0.6 m during December to 2.4 m in July (Anoop et al. 2014). The annual maximum SWH varies from 3.4 to 3.8 m in the eastern AS and from 2.7 to 6.3 m in the western BoB (Table 2). During 2010, the maximum measured SWH in a shallow water location was 3 m off Gangavaram and 2.7 m off Puducherry in the western BoB (Kumar et al. 2013a). During the same year, the maximum measured SWH was 4.2 m off Ratnagiri and 3.7 m off Honnavar in the eastern AS (Kumar et al. 2013a). During tropical cyclone (TC) Thane, a maximum SWH of 6 m was reported off Puducherry in the western BoB (Kumar et al. 2013b). The maximum measured SWH in the eastern AS was 5.9 m (Kumar et al. 2006) while the maximum measured SWH in the western BoB was 8.4 m during the passage of the Orissa super cyclone (Rajesh et al. 2005).

The scatter plot of the ERA-I SWH *versus* the buoy SWH and a least squares linear fit to the datasets is presented in Figure 2. The later shows that the slopes of the fit-line are predominantly close to 1 for locations along the west coast of India compared to locations along the east coast of India and a large deviation is observed for the location off Puducherry. The comparison statistics also illustrate that the ERA-I SWH data show good agreement with the buoy measured SWH data off the west coast of India (Table 2). The correlation coefficient (r) values for the SWH for the three observation stations off the west coast of India range from 0.96 to 0.98. The corresponding SI values range from 0.12 to 0.17 m whereas the RMSE values range from 0.18 to 0.29 m. The values of these three parameters highlight a good fit between the ERA-I data and the measured SWH data. A positive bias is found for the locations overall except for Ratnagiri where the ERA-I SWH values underestimate the corresponding associated observed SWH values.

The maximum buoy SWH (3.8 m) off Ratnagiri occurred in July during the SW monsoon and the corresponding ERA-I SWH was 3.1 m. During the period 2-3 September 2011, Ratnagiri was under the influence of TC Keila (IMD 2011). At 0000 UTC on 3 September 2011, the maximum buoy SWH was 3.7 m while the ERA-I SWH was 2.8 m, but at 0600 UTC, the ERA-I SWH (3.4 m) was close to the buoy SWH (3.6 m).

The monthly average values indicate that the difference between the ERA-I SWH and the buoy SWH is less along the west coast of India than along the east coast (Figure 3). Among the west coast locations, underestimation of the SWH in ERA-I is observed at the northern location (Ratnagiri), whereas overestimation of the SWH in ERA-I is observed at the other locations (Karwar and Honnavar). Karwar and Honnavar are swell-dominated locations (Sajiv et al. 2012; Anoop et al. 2014), and hence the overestimation of SWH in ERA-I at these locations is due to swell height overestimation since the swell dominance in the northern location is less than that at the southern locations (Kumar et al. 2014b). Aarnes et al. (2014) compared the ERA-I SWH with the measured data and reported that the largest bias in SWH is in the northeastern Atlantic. This is an effect of too weak wave growth off Newfoundland south of Cape Farewell and south of Iceland (areas with intense cyclone activity and often fetch-limited conditions). The SWH was overestimated by ERA-I in the eastern tropical Pacific Ocean and in the central Atlantic Ocean (areas dominated by swell) (Aarnes et al. 2014).

The difference between the ERA-I SWH and the buoy SWH varies from -1 to 1 m with an average value of -0.1 m for west coast locations (Figure 4). In contrast, this variation ranges from -2.2 to 1.7 m for east coast locations with an average value of -0.2 m (Figure 4). Even though the annual average values of bias indicate that ERA-I overestimates the SWH, it is found that the underestimation of SWH is large in ERA-I for a higher wave height (Figure 5). Off the west coast of India, waves with a SWH of more than 2 m are observed 10 to 15% of a year during the SW monsoon (Kumar and Anjali 2015). The locations off the west coast of India are strongly influenced by the SW monsoon, and hence two different patterns are observed in the difference between the ERA-I SWH and the buoy SWH, but the trend in underestimation/overestimation is the same during the monsoon and non-monsoon periods. The monthly bias values are small (< 0.2 m) off Ratnagiri and a relatively larger (0.2-0.5 m) bias is observed off Honnavar and Karwar during the SW monsoon period (Figure 6).

For the locations off the east coast of India, the scatter between the ERA-I SWH and the buoy SWH is large. It is largest for the location off Puducherry. Overestimation of the monthly mean SWH at all three locations off the east coast of India are observed in the ERA-I dataset since the waves were predominantly (84%) swells. The wave data of Gopalpur covers the data during TC Phailin (Nair et al. 2014). The maximum SWH from the buoy data during the TC is 6.3 m, whereas during the same period, the ERA-I data is 4.2 m and the underestimation of the SWH in ERA-I is ~33%. Due to low resolution, ERA-I underestimated the wave height at the peak of the cyclone. Shanas and Kumar (2014a) observed relatively high bias values for high waves (SWH > 2.5 m) for which the ERA-I data underestimated the measured SWH data up to 15%. The present study shows that the underestimation of the annual maximum SWH in ERA-I data along the west coast of India is less than 10%, whereas for the Puducherry and Gangavaram locations, the ERA-I data overestimates the annual maximum SWH by 12 and 46%, respectively (Table 3). Due to the formation of the cyclonic storm Laila over the southeast BoB during 17-20 May 2010 (Kumar et al. 2014a), a SWH up to 2.6 m was measured at 0000 UTC on 19 May 2010 and the corresponding ERA-I SWH was 3.1 m (indicating an overestimation of 19%).

The ERA-I 90th percentile value of the SWH for the west coast locations is within 10% of the measured values and the annual mean value, and the 75th percentile of the SWH shows variation up to 0.2 m.

The study shows that the ERA-I SWH can be used with a confidence of 85% for the shallow water locations off the west coast of India. However, for the locations off the east coast of India that are frequently influenced by TCs, ERA-I will underestimate the high SWH by a large percentage (~33%). Sandhya et al. (2014) observed that a SWH of 4.5 m was measured by a buoy during TC Nisha; whereas the estimated value based on WAVEWATCH III nested with SWAN was 2.8 m. The underestimation was due to the poor data quality of the input wind field used to force the wave model during extreme events. Nevertheless, considering that most of the wave modeling results show a difference between the measured and modeled SWH of up to 0.5-2 m, ERA-I can be used as a first hand information even for locations influenced by TCs.

The average SWH during February-October off Gopalpur (including a SWH of 6.3 m recorded during TC Phailin) is 1.3 m and the average SWH (excluding the TC) is 1.26 m (Kumar and Anoop, 2015). The

annual average SWH off Puducherry is 0.77 m including the SWH recorded during TC Thane (6 m) and the SWH recorded during periods excluding the TC (0.75 m) (Kumar et al. 2013b). Even though large wave heights are generated during TCs, the influence of a TC on the annual average SWH is not significant since the influence of the cyclone lasts only 3 to 4 days (Amrutha et al. 2014). Since the annual mean SWHs are not significantly influenced by TCs, the annual mean ERA-I SWH data for the region influenced by a TC can be used for further studies since ERA-I underestimates only the SWH in upper percentiles (Stopa and Cheung 2014). The study shows that ERA-I SWH can be used with confidence for locations which are least influenced by TCs.

b. Wave period

The comparison of the ERA-I wave period with the mean wave period (T_{m02}), zero crossing wave period (T_z), wave period corresponding to the mean frequency of the wave spectrum (T_{m01}) and energy wave period (T_e) showed that the energy wave period is close to the ERA-I wave period (figures not presented). Hence, further analysis was carried out using the energy wave period (T_e) and the ERA-I wave period.

The correlation coefficient (r) values between the ERA-I T_e and the buoy T_e for three locations along the west coast of India are 0.96 to 0.98. Lower values of SI (0.12 to 0.17 s) are found for these locations, which indicate a good fit between the ERA-I T_e and the buoy T_e (Figure 6). The difference between the ERA-I T_e and the buoy T_e varies from -6 to 4 s with an average value of -0.3 s (Figure 7). For locations off the west coast of India, the difference between the buoy T_e and the ERA-I T_e is large (> 2 s) during the non-monsoon period due to the sea/land breeze influence in the coastal areas (Glejin et al. 2013a). The difference between the buoy T_e and the ERA-I T_e is large (> 2 s) when the wave height is less ($SWH < 1.5$ m). For locations off Gangavaram, the average difference between the buoy T_e and the ERA-I T_e is large (~ 1.8 s) compared to other locations (< 0.3 s). The 90th percentile value of T_e is within 10% except for the buoy off Gangavaram (Table 4).

Wave data in ERA-I were produced on a grid with a resolution of the order of 110 km. Even though shallow water physics are active in the model, due to the coarseness of the grid, the coupled wave component (Janssen 2004) is coarser at approximately 110 km and the mean water depth at the point of interest is different from the buoy location. Also, the data used for evaluating the ERA-I data in the

present study were collected using buoys located 1.5 to 5 km from the coast (Table 1). This difference in water depth might explain the discrepancies between the ERA-I observations and the buoy observations, in particular in terms of wave period.

4. Summary and conclusions

In this study, we evaluated the performance of ECMWF Interim Re-Analysis SWH and Te data at six shallow water locations around the Indian sub-continent by comparing data from these locations with in-situ buoy measurements. Three locations along the west coast and three locations along the east coast of India were selected. Measured data covering different seasons were used for the study.

The analysis showed that ERA-I overestimates the SWH along the west coast of India due to swell height overestimation. The difference between the ERA-I SWH and the buoy SWH is up to 15% for shallow water locations off the west coast of India. Even though the annual average values of bias indicate that ERA-I overestimates the SWH, underestimation of the SWH is large in ERA-I for higher wave heights (> 2.5 m). The locations off the east coast of India are frequently influenced by TCs, and ERA-I underestimates the SWH at these locations during the cyclone period by 33%. Hence, ERA-I should not be used for design applications without proper validation. The difference between the buoy Te and the ERA-I Te is large (> 2 s) when the SWH is less than 1.5 m.

In summary, it is difficult to assess the root causes of ERA-I biases and errors using a low-resolution global model in a somewhat complex basin (primarily, the Bay of Bengal) with in situ observations located in the nearshore environment. Orographic effects and bathymetry may be at play in this environment. Given this, one would expect to find lowest confidence in the ERA-I data at the Puducherry site, where partial obstruction from southerly wave energy comes into play as well as the potential for land-sea interaction with planetary boundary layer wind flow. As indicated, the model results from the onshore monsoonal flow are better depicted by ERA-I. Thus, stratifying results into seasonal categories is an appropriate strategy and explains the superior results along the west coast. However, short-term sub-synoptic scale wind pulses and fluctuations are not likely to be captured by a lower resolution ERA-I.

Acknowledgments

The authors acknowledge the Earth System Science Organization (ESSO)-Indian National Centre for Ocean Information Services (INCOIS), Ministry of Earth Sciences, Government of India for funding the wave measurement program and Council of Scientific and Industrial Research, New Delhi for funding the research work. Director, CSIR-NIO, Goa provided encouragement to carry out the study. We thank Dr. T.M. Balakrishnan Nair, Head, OSISG and Mr. Arun Nherakkol, Scientist, INCOIS, Hyderabad and Mr. Jai Singh, Technical Assistant, CSIR-NIO for help during the data collection and Mr.T.R.Anoop for data analysis. ERA-Interim data used in this study have been obtained from the ECMWF data server: <http://data.ecmwf.int/data>. We thank the two reviewers for the constructive comments and suggestions that substantially improved the paper. This is NIO contribution No. ***.

References

- Aarnes, O.J., S. Abdalla, J. Bidlot, and Ø. Breivik, 2014: Marine wind and wave height trends at different ERA-Interim forecast ranges. *J. Climate*, **28**, 819-837. doi: 10.1175/JCLI-D-14-00470.1
- Agarwal, A., V. Venugopal, and G. P. Harrison, 2013: The assessment of extreme wave analysis methods applied to potential marine energy sites using numerical model data, *Renewable Sustainable Energy Rev.*, **27**, 244–257.
- Amrutha, M.M., V.S. Kumar, T.R. Anoop, T.M.B. Nair, A. Nherakkol, and C. Jeyakumar, 2014: Waves off Gopalpur, Northern Bay of Bengal during the cyclone PHAILIN, *Ann. Geophys.*, **32**, 1073-1083.
- Anoop, T. R., V.S. Kumar, and P.R. Shanab, 2014: Spatial and temporal variation of surface waves in shallow waters along eastern Arabian Sea, *Ocean Eng.*, **81**, 150-157, doi: 10.1016/j.oceaneng.2014.02.010.
- Bidlot, J.R., P.A.E.M. Janseen, S. Abdalla, and H. Hersbach, 2007: A revised formulation of ocean wave dissipation and its model impact, *ECMWF Technical Report Memorandum*, 509. European Centre for Medium-Range Weather Forecasting, Reading, UK, 27p.
- Caires, S., and A. Sterl, 2005: A new non-parametric method to correct model data: Application to significant wave height from the ERA-40 reanalysis. *J. Atmos. Oceanic Technol.*, **22**, 443-459.
- Dee D. P., and Coauthors, 2011: The ERA-Interim reanalysis: configuration and performance of the data assimilation system. *Q. J. R. Meteorol. Soc.*, **137**, 553–597, DOI: 10.1002/qj.828.
- Dora, G.U, and V.S. Kumar, 2015: Sea state observation in island sheltered nearshore zone based on in-situ intermediate-water wave measurements and NCEP/CFSR wind data, *Ocean Dynamics* (in press). DOI: 10.1007/s10236-015-0822-1.

Glejin, J., V. S. Kumar, and T. M. B. Nair, 2013b: Monsoon and cyclone induced wave climate over the near shore waters off Puduchery, south western Bay of Bengal. *Ocean Eng.*, **72**, 277-286, <http://dx.doi.org/10.1016/j.oceaneng.2013.07.013>.

Glejin, J., V. S. Kumar, T. M. B. Nair, and J. Singh, 2013a: Influence of winds on temporally varying short and long period gravity waves in the near shore regions of the eastern Arabian Sea. *Ocean Science*, **9**, 343–353.

Gulev, S.K., V. Grigorieva, 2004: Last century changes in ocean wind wave height from global visual wave data. *Geophys. Res. Lett.*, **31**, L24302, doi: 10.1029/2004GL021040.

IMD, 2011, Cyclonic storm 'KEILA' over the Arabian Sea (29 October- 04 November, 201, <http://www.imd.gov.in/section/nhac/dynamic/CSKeila29Oct-4Nov2011.pdf>, accessed on 3 August 2014.

Janssen P. A. E. M., 2008: Progress in ocean wave forecasting. *J. Comput. Phys.*, **227**, 572–3594.

Janssen P. A. E. M., J. R. Bidlot, S. Abdalla, and H. Hersbach, 2005: Progress in ocean wave forecasting at ECMWF. *Tech. Memo.* 478, ECMWF: Reading, UK

Janssen, P.A.E.M., 2004: The Interaction of Ocean Waves and Wind. Cambridge University Press, Cambridge, UK, 312 pp.

Komen G. J., L. Cavaleri, M. Doneland, K. Hasselmann, S. Hasselmann, and P. A. E. M. Janssen, 1994: Dynamics and Modelling of Ocean Waves. Cambridge University Press, Cambridge, UK.

Kumar, V. S., K. K. Dubhashi, and T. M. B. Nair, 2014a: Spectral wave characteristics off Gangavaram, East coast of India, *J. Oceanogr.*, **70**, 307–321, DOI 10.1007/s10872-014-0223-y.

Kumar, V. S., P. R. Shanas, and K. K. Dubhashi, 2014b: Shallow water wave spectral characteristics along the eastern Arabian Sea, *Natural Hazards*, **70**, 377–394, DOI 10.1007/s11069-013-0815-7.

Kumar, V.S., and M. Anjali Nair, 2015: Inter-annual variations in wave spectral characteristics at a location off the central west coast of India, *Ann. Geophys.*, **33**, 159-167. doi:www.ann-geophys.net/33/159/2015/.

Kumar, V.S., and T.R. Anoop, 2015: Spatial and temporal variations of wave height in shelf seas around India, *Natural Hazards* (under review).

Kumar, V.S., J. Glejin, K.K. Dubhashi, and T.M.B. Nair, 2013b: Waves during THANE cyclone, Bay of Bengal, *Natural Hazards*, **69**, 509-522. doiI 10.1007/s11069-013-0713-z.

Kumar, V.S., K.C. Pathak, P. Pednekar, N.S.N. Raju, and R. Gowthaman, 2006: Coastal processes along the Indian coastline, *Curr. Sci.*, 91(4), 530-536.

Kumar, V.S., K.K. Dubhashi, T.M.B. Nair, and J. Singh, 2013a: Wave power potential at few shallow water locations around Indian coast. *Curr. Sci.*, **104**, 1219-1224.

Nair, T. M. B., P. G. Remya, R. Harikumar, K. G. Sandhya, P. Sirisha, K. Srinivas, C. Nagarju, A. Nherakkol, B. K. Prasad, C. Jeyakumar, K. Kaviyazhahu, N. K. Hithin, R. Kumari, V. S. Kumar, M. R. Kumar, S. S. C. Sheno, and S. Nayak, 2014: Wave forecasting and monitoring during Very Severe Cyclone Phailin in the Bay of Bengal, *Curr. Sci.*, **106**, 1121-1125.

- Portilla, J., J. Sosa, and L. Cavaleri, 2013: Wave energy resources: Wave climate and exploitation, *Renewable Energy*, **57**, 594-605.
- Rajesh, G., K. JossiaJoseph, M. Harikrishnan, and K. Premkumar, 2005: Observations on extreme meteorological and oceanographic parameters in Indian seas, *Curr. Sci.*, **88**, 1279–1282.
- Remya, P. G., Rajkumar, S. Basu and A. Sarkar, 2012: Wave hindcast experiments in the Indian Ocean using MIKE 21 SW model, *J. Earth Syst. Sci.* **121** (2), 385–392.
- Sajiv, P. C., V. S. Kumar, J. Glejin, G. U. Dora, and P. Vinayaraj, 2012: Interannual and seasonal variations in near shore wave characteristics off Honnavar, west coast of India, *Curr. Sci.*, **103**, 286-292.
- Sandhya, K. G., T. M. B. Nair, P. K. Bhaskaran, L. Sabique, N. Arun, and K. Jeykumar, 2014: Wave forecasting system for operational use and its validation at coastal Puducherry, east coast of India, *Ocean Eng.*, **80**, 64-7.
- Shanas, P. R. and V. S. Kumar, 2014b: Temporal variations in the wind and wave climate at a location in the eastern Arabian Sea based on ERA-Interim reanalysis data, *Natural Hazards and Earth System Sciences*, **14**, 1371–1381, doi:10.5194/nhess-14-1371-2014.
- Shanas, P. R., and V. S. Kumar, 2014a: Comparison of ERA-Interim waves with buoy data in the eastern Arabian Sea during high waves, *Indian J. Mar. Sci.*, **43**, (in press).
- Shanas, P.R., and V.S. Kumar, 2015: Trends in surface wind speed and significant wave height as revealed by ERA-Interim wind wave hindcast in the Central Bay of Bengal, *International Journal of Climatology*, doi: 10.1002/joc.4164 (available online).
- Singh, O.P., T.M.A. Khan, and S. Rahman, 2000: Changes in the frequency of tropical cyclones over the North Indian Ocean, *Meteorol. Atmos. Phys.*, **75**, 11–20.
- Slingo, J., H. Spencer, B. Hoskins, P. Berrisford, and E. Black, 2005: The meteorology of the Western Indian Ocean and the influence of the East African Highlands, *Phil. Trans. R. Soc. A.*, **363**, 25-42, doi: 10.1098/rsta.2004.1473.
- Stopa, J. E., and K. F. Cheung, 2014: Intercomparison of wind and wave data from the ECMWF Reanalysis Interim and the NCEP Climate Forecast System Reanalysis, *Ocean Modell.*, **75**, 65-83, doi: 10.1016/j.ocemod.2013.12.006.
- Traon, P. Y. L., 2013: From satellite altimetry to Argo and operational oceanography: three revolutions in oceanography, *Ocean Sci.*, **9**: 901–915, doi:10.5194/os-9-901-2013.
- Tucker, M.J., and E.G.Pitt, 2001: *Waves in Ocean Engineering*. Elsevier New York, p. 521.
- Vethamony, P., K. Sudheesh, S. P. Rupali, M. T. Babu, S. Jayakumar, A. K. Saran, S. K. Basu, R. Kumar and A. Sarkar, 2006: Wave modelling for the north Indian Ocean using MSMR analysed winds, *International Journal of Remote Sensing*, **27** (18), 3767-3780.

Figure captions

Figure 1. Map showing the shallow water locations considered in the study

Figure 2. Scatter plot of ERA-I SWH with buoy SWH for different locations. The plot also shows the linear fit and the 85% confidence limit

Figure 3. Left panel shows the average value of SWH for each month from ERA-I and Buoy and right panel shows the average value of energy wave period for each month from ERA-I and Buoy at all the locations considered in the study

Figure 4. Time series plot of the difference between ERA-I SWH and buoy SWH at different locations

Figure 5. Scatter plot of difference between ERA-I SWH and buoy SWH with buoy SWH during monsoon and non-monsoon period at all locations

Figure 6. Biases and correlation coefficient between ERA-I SWH and buoy SWH for each month. Left panel shows the locations off the west coast of India and the right panel for the locations off the east coast of India

Figure 7. Scatter plot of ERA-I wave period (T) with buoy energy wave period (T_e) for different locations

Figure 8. Time series plot of the difference between ERA-I wave period (T) and buoy energy wave period (T_e) at different locations

Table 1. Measurement locations and the water depth

Location	Latitude	Longitude	Water depth (m)	Distance from coast (km)	Period of validation
off Ratnagiri, west coast	16.980° N;	73.258° E	13	2.0	1 January 2011 to 31 December 2011
off Karwar, west coast	14.822° N;	74.052° E	15	5.0	1 January 2011 to 31 December 2011
off Honnavar, west coast	14.304° N;	74.391° E	9	2.5	1 January 2011 to 31 December 2011
off Puducherry, east coast	11.925° N;	79.851° E	12	2.0	1 January 2010 to 31 December 2010
off Gangavaram, east coast	17.632° N;	83.265° E	18	2.0	1 January 2010 to 31 December 2010
off Gopalpur, east coast	19.282° N;	84.964° E	15	1.5	1 February 2013 to 10 October 2013

Table 2. Comparison statistics of buoy data and ERA-I data for significant wave height and energy wave period

	Ratnagiri	Karwar	Honnava r	Puducherry	Gangavaram	Gopalpur
Number of data	1459	1459	1452	1459	1423	1015
Significant wave height						
r	0.98	0.98	0.96	0.71	0.91	0.90
RMSE (m)	0.18	0.23	0.29	0.4	0.36	0.29
Bias (m)	-0.09	0.17	0.2	0.31	0.28	0.16
SI	0.15	0.12	0.17	0.24	0.18	0.17
Energy wave period						
r	0.83	0.72	0.65	0.61	0.68	0.87
RMSE (s)	0.94	1.16	1.37	1.18	1.48	0.98
Bias (s)	0.08	-0.21	-0.33	0.13	-0.88	-0.25
SI	0.13	0.14	0.16	0.18	0.15	0.11

Table 3. Annual mean, annual maximum, 75th and 90th percentile of SWH from buoy and ERA-I

Location	Annual mean (m)		75 th percentile (m)		90 th percentile (m)		Annual maximum (m)	
	Buoy	ERA-I	Buoy	ERA-I	Buoy	ERA-I	Buoy	ERA-I
off Ratnagiri	1.1	1.0	1.7	1.6	2.3	2.2	3.8	3.4
off Karwar	1.1	1.3	1.7	2.0	2.4	2.6	3.9	3.8
off Honnavar	1.0	1.2	1.4	1.9	2.2	2.4	3.7	3.6
off Puducherry	0.7	1.0	0.8	1.2	1.0	1.4	2.4	2.7
off Gangavaram	1.0	1.3	1.3	1.6	1.6	2.0	2.6	3.8
off Gopalpur	1.3	1.5	1.6	1.7	1.9	2.1	6.3	4.2

Table 4. Annual mean, annual maximum, 75th and 90th percentile of energy wave period from buoy and ERA-I

Location	Annual mean (s)		75 th percentile (s)		90 th percentile (s)		Annual maximum (s)	
	Buoy	ERA-I	Buoy	ERA-I	Buoy	ERA-I	Buoy	ERA-I
off Ratnagiri	7.3	7.4	8.5	8.6	9.2	9.1	14.4	11.8
off Karwar	8.1	7.9	9.0	9.0	10.1	9.4	14.7	12.2
off Honnavar	8.6	8.3	9.5	9.2	10.8	9.7	15.1	12.4
off Puducherry	6.3	6.5	7.3	7.2	8.2	8.1	11.4	12.9
off Gangavaram	9.5	7.7	10.6	8.6	11.5	9.4	14.7	12.1
off Gopalpur	8.6	8.4	9.9	9.4	11.2	10.3	15.5	13.8

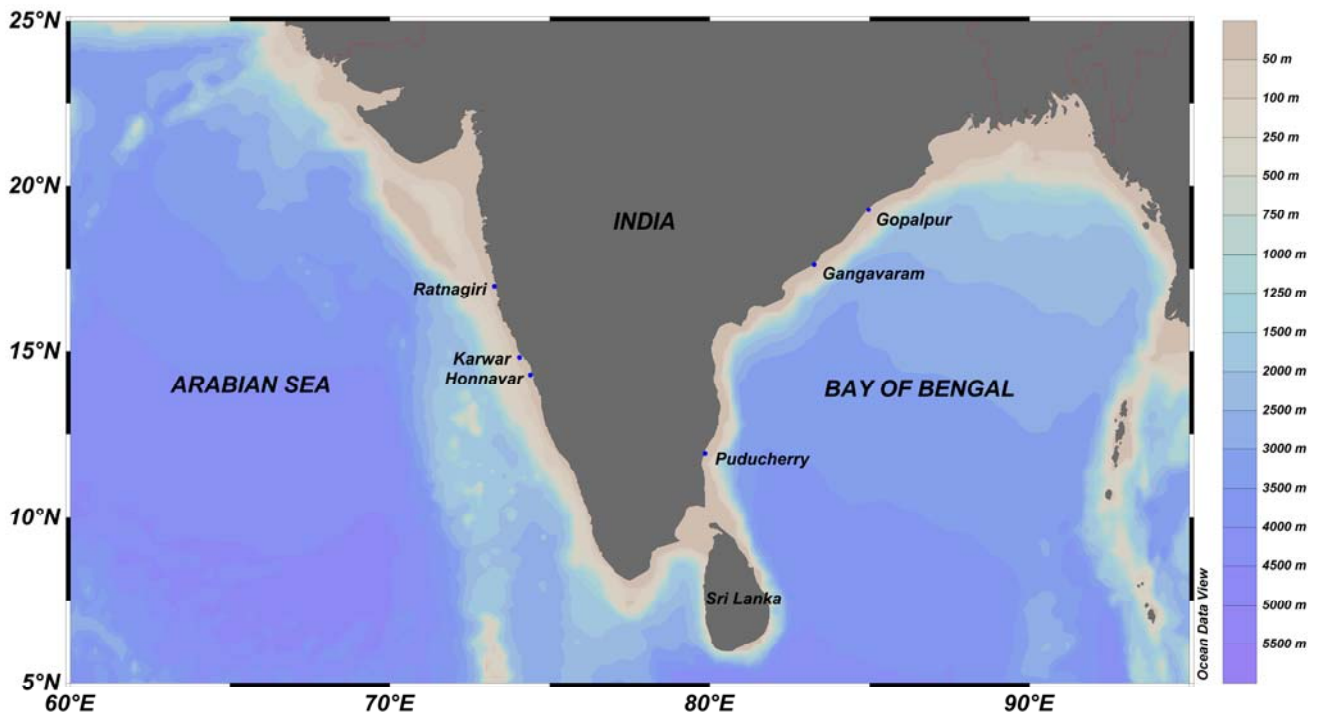


Figure 1. Map showing the shallow water locations considered in the study

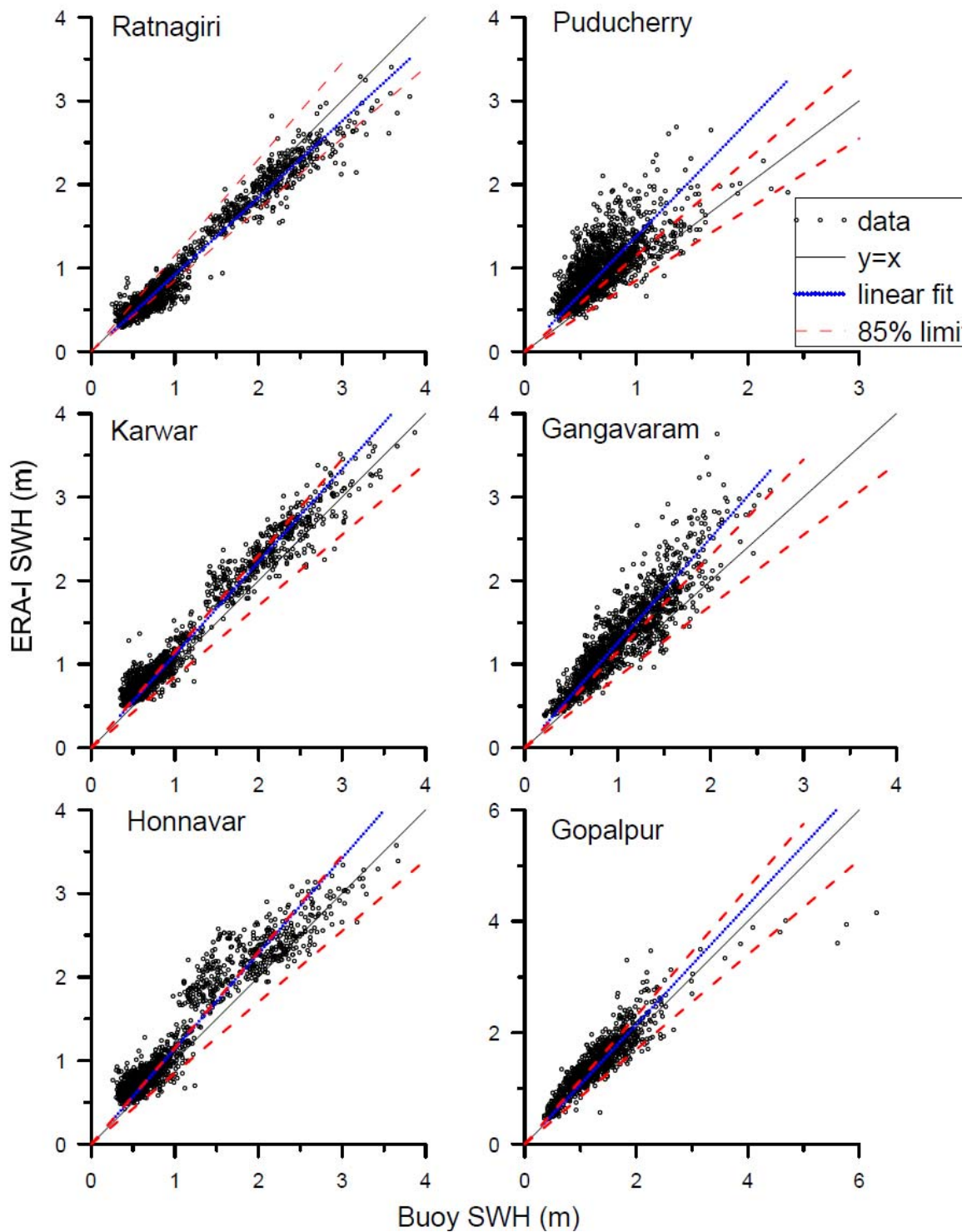


Figure 2. Scatter plot of ERA-I SWH with buoy SWH for different locations. The plot also shows the linear fit and the 85% confidence limit

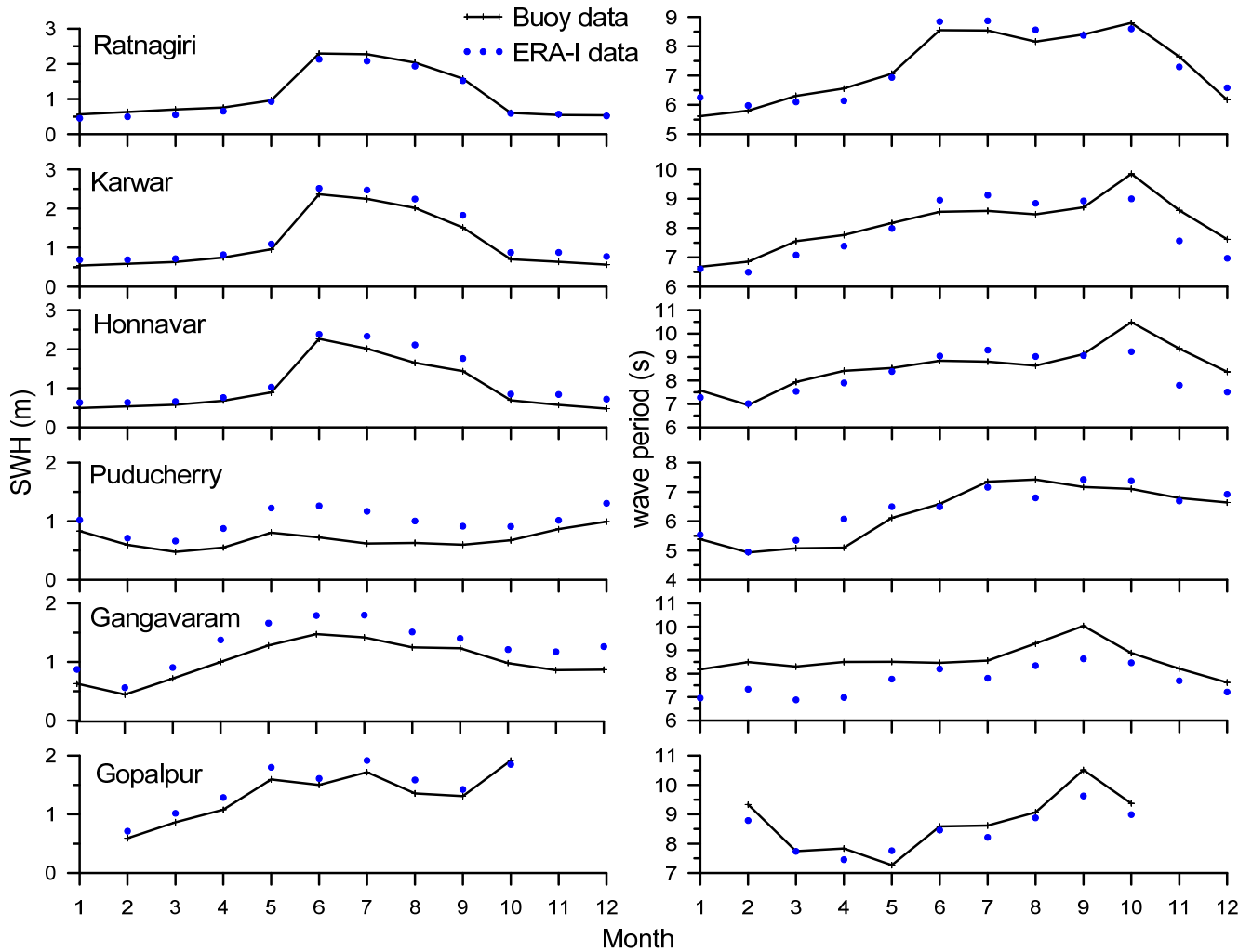


Figure 3. Left panel shows the average value of SWH for each month from ERA-I and Buoy and right panel shows the average value of energy wave period for each month from ERA-I and Buoy at all the locations considered in the study

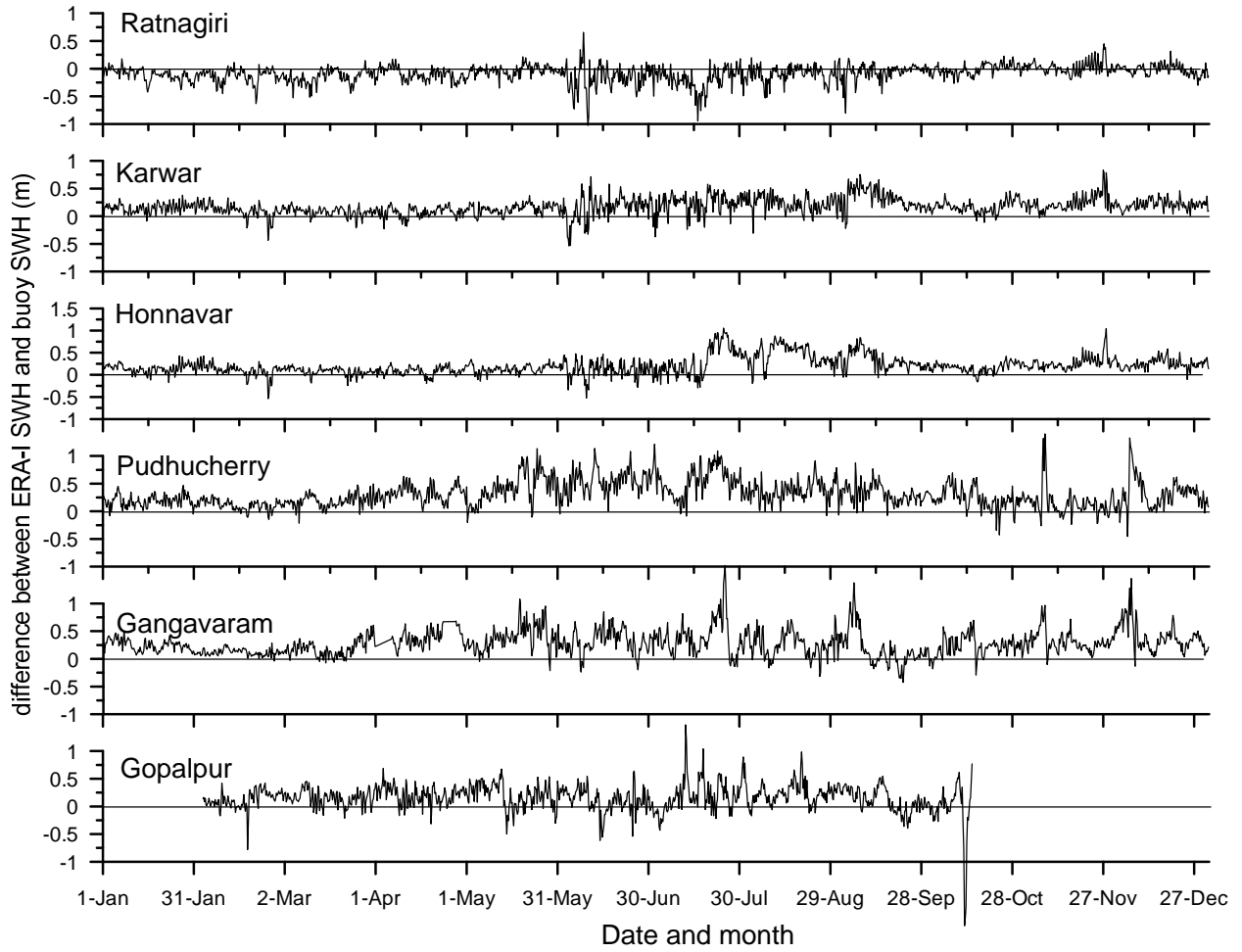


Figure 4. Time series plot of the difference between ERA-I SWH and buoy SWH at different locations

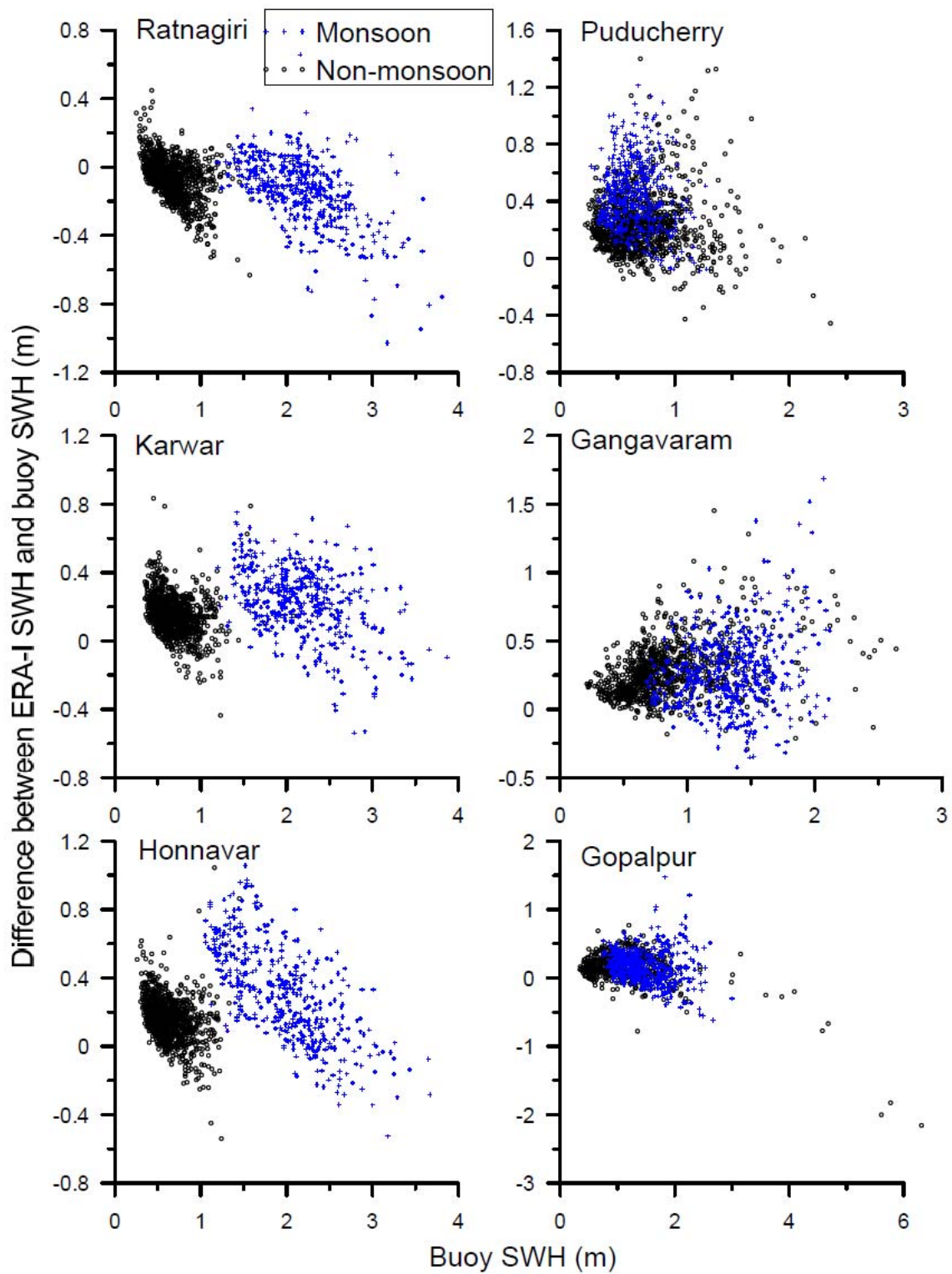


Figure 5. Scatter plot of difference between ERA-I SWH and buoy SWH with buoy SWH during monsoon and non-monsoon period at all locations

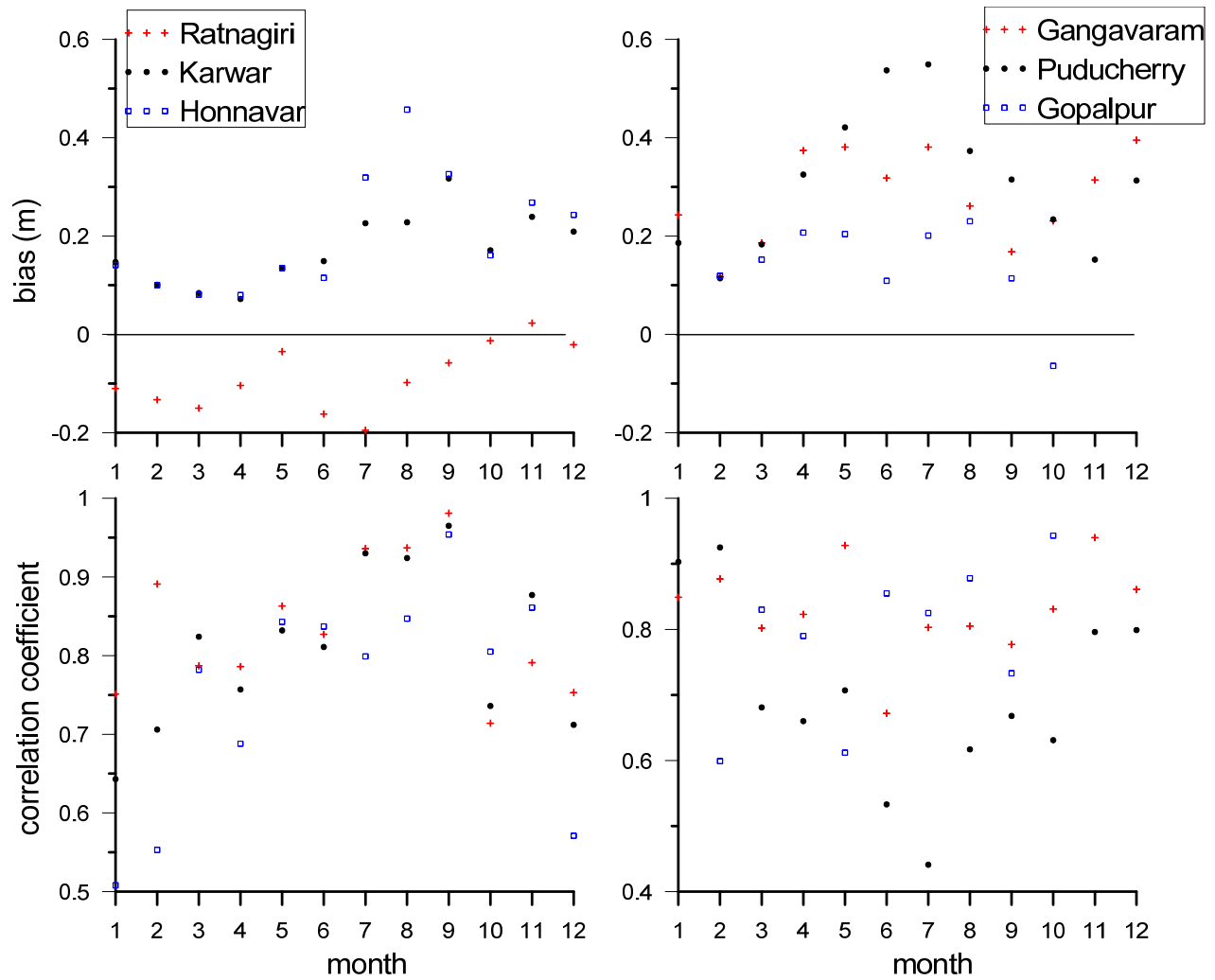


Figure 6. Biases and correlation coefficient between ERA-I SWH and buoy SWH for each month. Left panel shows the locations off the west coast of India and the right panel for the locations off the east coast of India

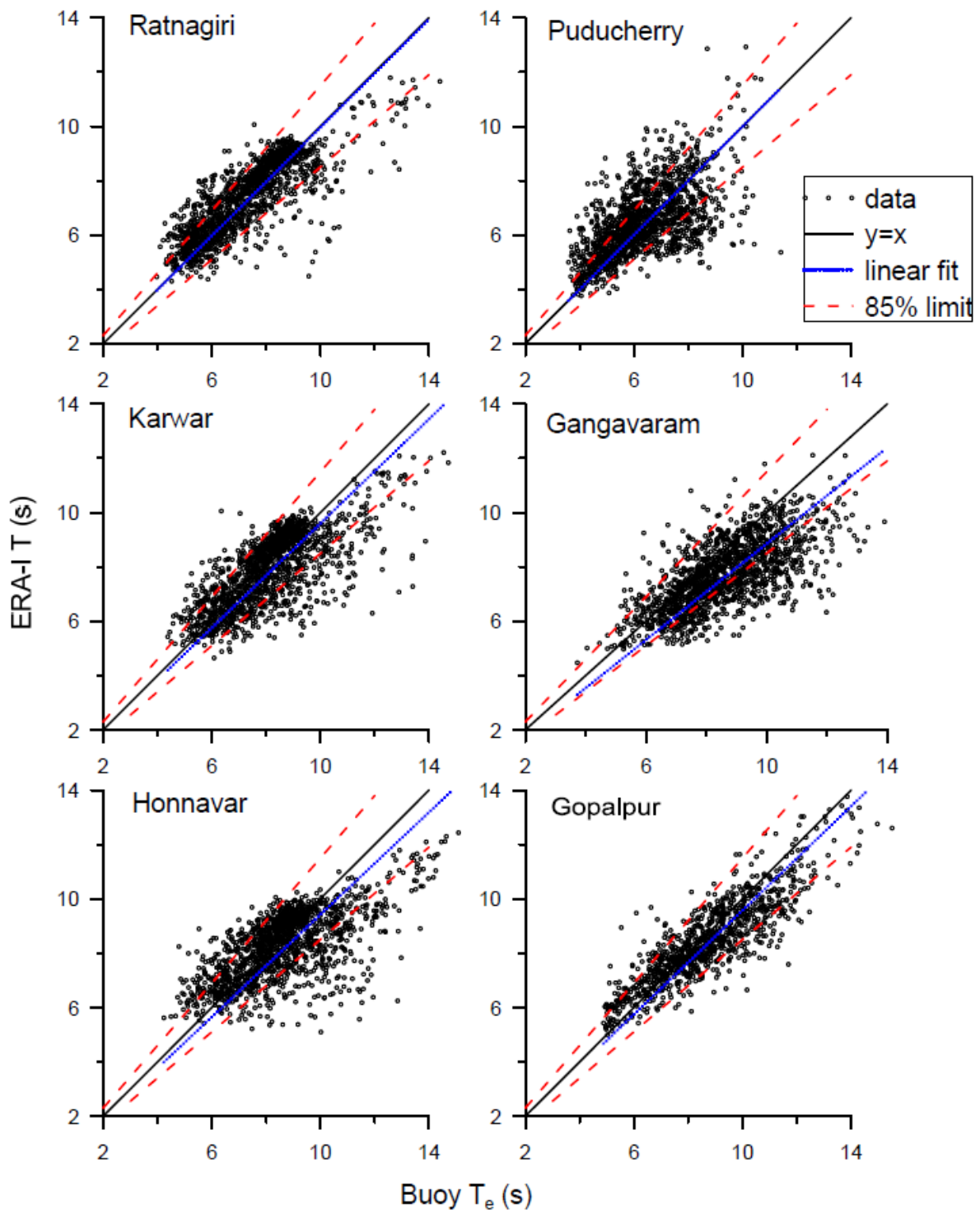


Figure 7. Scatter plot of ERA-I wave period (T) with buoy energy wave period (T_e) for different locations

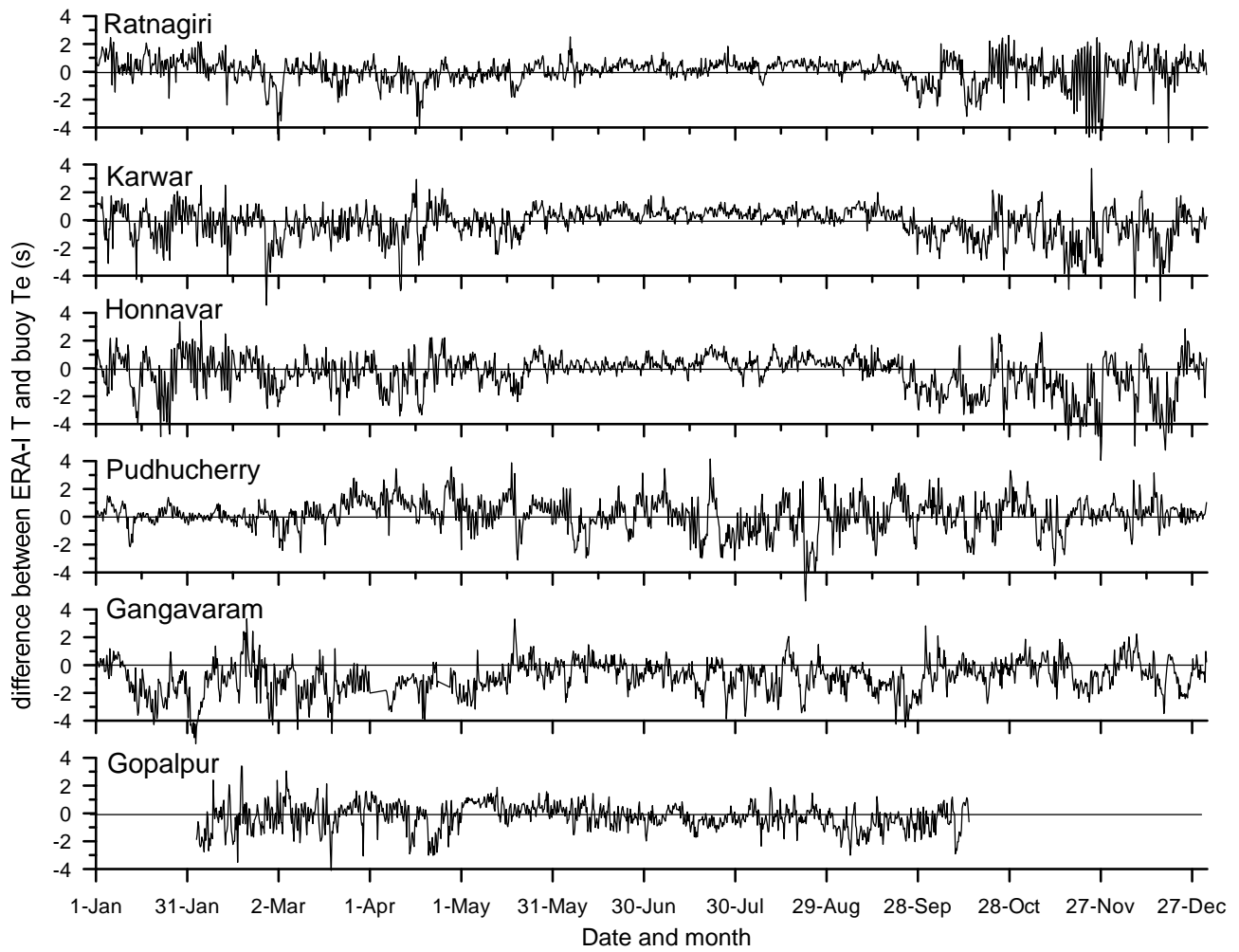


Figure 8. Time series plot of the difference between ERA-I wave period (T) and buoy energy wave period (Te) at different locations